IOPscience iopscience.iop.org

Home Search Collections Journals About Contact us My IOPscience

Imaging random telegraph signal sites near a quasi 1D electron system

This article has been downloaded from IOPscience. Please scroll down to see the full text article.

2001 J. Phys.: Condens. Matter 13 L249

(http://iopscience.iop.org/0953-8984/13/11/105)

View the table of contents for this issue, or go to the journal homepage for more

Download details:
IP Address: 171.66.16.209
The article was downloaded on 14/05/2010 at 16:35

Please note that terms and conditions apply.

INSTITUTE OF PHYSICS PUBLISHING JOURNAL OF PHYSICS: CONDENSED MATTER

J. Phys.: Condens. Matter **13** (2001) L249–L254 www.iop.org/Journals/cm PII: S0953-8984(01)20424-X

LETTER TO THE EDITOR

Imaging random telegraph signal sites near a quasi 1D electron system

R Crook, C G Smith, M Y Simmons[1] and D A Ritchie

Department of Physics, Cavendish Laboratory, Madingley Road, Cambridge, CB3 OHE, UK

E-mail: rc230@cam.ac.uk (R Crook)

Abstract

Conductance of a quasi 1D electron system (Q1DES) is a sensitive detector of the local electric potential. Electrons hopping between defect states can generate a random telegraph signal in conductance measurements made against time. Such a detector, defined in a GaAs/AlGaAs heterostructure, was used to generate images of the electric potential of a scanning charged tip and structure seen in the Q1DES conductance images is consistent with an electron hopping between two defect states separated by slightly more than the Bohr orbit. The occupation probability being mediated by the position of the scanning tip over the defect near the Q1DES. Images suggest that a puddle of mobile charge in the donor layer can screen the tip from the defect system.

Switching between conductance values has previously been observed in quasi 1D electron systems (Q1DES) as a function of time [1–4], where it was referred to as a random telegraph signal (RTS). The two states of a binary RTS were interpreted as the probabilistic exchange of an electron between the adjoining 2D electron system (2DES) and a nearby defect state, so altering the Q1DES conductance by coulombic interaction. When the measurement time constant is longer than the switching period, a time average of the RTS is measured. If the occupation probability of the switching sites is gradually changed, by varying the width of the Q1DES for example, then a smooth time averaged structure is observed [1]. Multiple level defect systems give rise to multiple level switching, and the occupation of one defect state may by influenced by the occupation of another nearby defect state [2, 4]. At the low temperatures used in these experiments electron movement is almost always by tunnelling because thermal excitation to defect states becomes improbable.

In this letter we report scanned gate microscopy experiments [5–9], where a charged probe scanned over a Q1DES. To generate the conductance images presented in this letter, the Q1DES conductance was recorded to determine the image contrast as the tip scanned over a rectangular region. The charged probe was a modified low-temperature atomic force microscope (AFM) using a piezoresistive cantilever to support a conductive tip. Q1DES conductance is a sensitive probe of the local electric potential [10], so the images reveal the electric potential of the charged tip. Superimposed on the images were regions of increased or decreased conductance, due to the binary switching of a local defect system being detected by the Q1DES. The defect

[1] Present address: School of Physics, University of New South Wales, Sydney 2052, Australia.

state occupancy was evidently modified by the tip position. These images therefore provide information about the position and origin of switching centres.

A 2DES was formed at a GaAs/AlGaAs heterojunction 98 nm beneath the device surface, with 12×10^{18} cm^{-3} Si doping from 40 nm to 80 nm above the 2DES. Negatively biased surface electrodes depleted the underlying 2DES to define the Q1DES. The 30 nm thick surface electrodes were in a split-gate configuration with a lithographic width and length of 700 nm. Figure 1(a) plots Q1DES conductance against gate bias at 1.5 K. The conductance is quantized in approximate units of $2e^2/h$, demonstrating the 1D nature of the device.

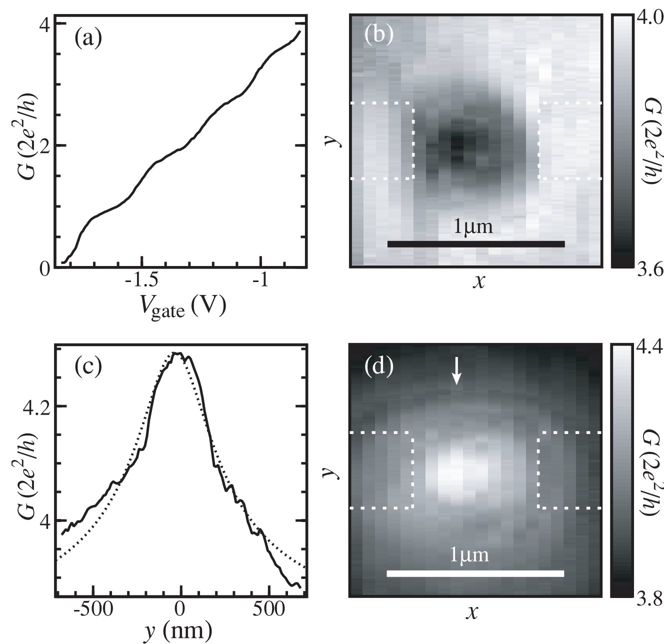

Figure 1. (a) Plot of Q1DES conductance against gate bias, at 1.5 K. No correction has been made for series resistance. (b) Q1DES conductance image with $V_{\rm tip} = -1.5$ V. The surface electrodes are outlined. (c) Model (dotted) and experimental (solid) single sweep reproduced from conductance image (d) where $V_{\rm tip} = +1.5$ V.

The scanning probe was a modified low-temperature AFM with a conductive tip. A piezoresistive cantilever [11] [2] was used to measure the force between the tip and the surface, avoiding the complications of using an optical measurement system with light sensitive devices at low temperatures. To locate the split-gate surface electrodes the AFM was used in topographic mode, where images of an alignment grid provided orientation. To produce conductance images the AFM force feedback circuit was disconnected and the tip scanned in a plane 60 nm above the GaAs surface at a speed of 9.6 nm s^{-1}. A DC bias was applied to the cantilever which had a resistive path to the conductive tip.

Figures 1(b) and 1(d) show conductance images where switching is not significant. In figure 1(b) the DC tip bias was $V_{\rm tip} = -1.5$ V, while in figure 1(d) $V_{\rm tip} = +1.5$ V. The Q1DES conductance was measured by applying a low-frequency AC signal of 0.1 mV to the Q1DES source while recording the AC Q1DES drain current with a lock-in amplifier. The images reveal the tip perturbing potential in the 2DES layer. The solid line in figure 1(c) plots a single

[2] Park Scientific Instruments, Sunnyvale, CA 94089, USA.

sweep from the image in figure 1(d) where it is identified by an arrow.

To quantify the screening effect from surface and donor states, a model is now discussed. By modelling the tip as a charged sphere of radius r_{tip} and ignoring screening, the tip perturbing potential in the 2DES plane takes the functional form

$$\left(\rho^2 + (d + r_{tip})^2\right)^{-0.5} \tag{1}$$

where ρ is the radial distance in the 2DES plane and d is the distance from the tip to the 2DES. The dashed line in figure 1(c) is this function fitted to the experimental data with $r_{tip} = 130$ nm in agreement with AFM images. The peak potential occurs in a region of low radial potential gradient, so this region is approximated as a parallel plate capacitor, ignoring edge effects. From the classical result that $\Delta G/G_0 = \Delta n/n_0$ where G_0 is the conductance at channel definition and n_0 is the 2DES carrier concentration, the change in conductance ΔG is derived as [12]

$$\Delta G = \frac{\epsilon_0(V_{tip} + V_{contact})G_0}{en_0}\left(\frac{d_{He}}{\epsilon_{He}} + \frac{d_{AlGaAs}}{\epsilon_{AlGaAs}}\right)^{-1}. \tag{2}$$

The contact potential $V_{contact}$ is approximately -0.4 V. The dielectric has two layers: $\epsilon_{He} = 1$, $d_{He} = 60$ nm for the helium filled gap between the tip and surface; $\epsilon_{AlGaAs} = 12.9$, $d_{AlGaAs} = 98$ nm for the device material between the surface and the 2DES. At the peak conductance, the experimental ΔG is 40 μS being seven times smaller than the value calculated from equation (2). This is a measure of screening from electrons in the high density of GaAs surface states and free electrons in the doped AlGaAs layer [13]. The classical approximation for conductance is applicable because the measurements were made with between three and four occupied 1D subbands, and where the quantized conductance was weak.

The device used to generate figure 1 was then illuminated with a red light emitting diode. Figure 2(a) plots Q1DES conductance up to the second 1D plateau. An arrow identifies a small 'plateau feature' characteristic of switching, where the gate bias modifies the occupation probability of defect states. Figure 2(b) shows a conductance image made immediately after figure 2(a) with the tip scanning 60 nm off the surface and $V_{tip} = -0.5$ V. The defect state occupation probability is also modified by the tip position. This is observed as a distinct region of increased conductance superimposed upon a tip potential image similar to figure 1(b). The approximate boundary of the region of increased conductance is identified by a black line. Each image took about one hour to generate, during which the Q1DES conductance can drift slightly. This caused a small x direction slope to be superimposed on the image in figure 2(b), but did not affect the switching features. Figure 2(c) plots a single sweep from figure 2(b) where it is identified by an arrow. The switching observed in figures 2(a) and 2(b) is believed to originate from the same defect system.

From comparison with similar devices [14], a change of 1 V in gate bias corresponds to an approximate 13 meV change in the Q1DES potential. The conductance step in figure 2(b) is constant and corresponds to 3.8 μS, which would require a change of 9.3 mV in the gate bias to achieve the same change in conductance. From the ratio relating gate bias to Q1DES potential, an energy change of 120 μeV is assigned to this switch.

The origin of the switch is first assumed to be the exchange of a single electron between the 2DES and a defect state. By modelling the electron as a point source, the distance from the defect to the Q1DES is approximately 1 μm [1]. This figure is an overestimate due to screening from the 2DES and free electrons in the donor layer. However, the conductance image of figure 2(b) suggests that the defect is located approximately 100 nm from the Q1DES. This discrepancy questions this model as the origin of the switch.

Instead, it is proposed that the origin of this switch is the exchange of a single electron between two defect states in the donor layer. Using this model, possible defect locations were

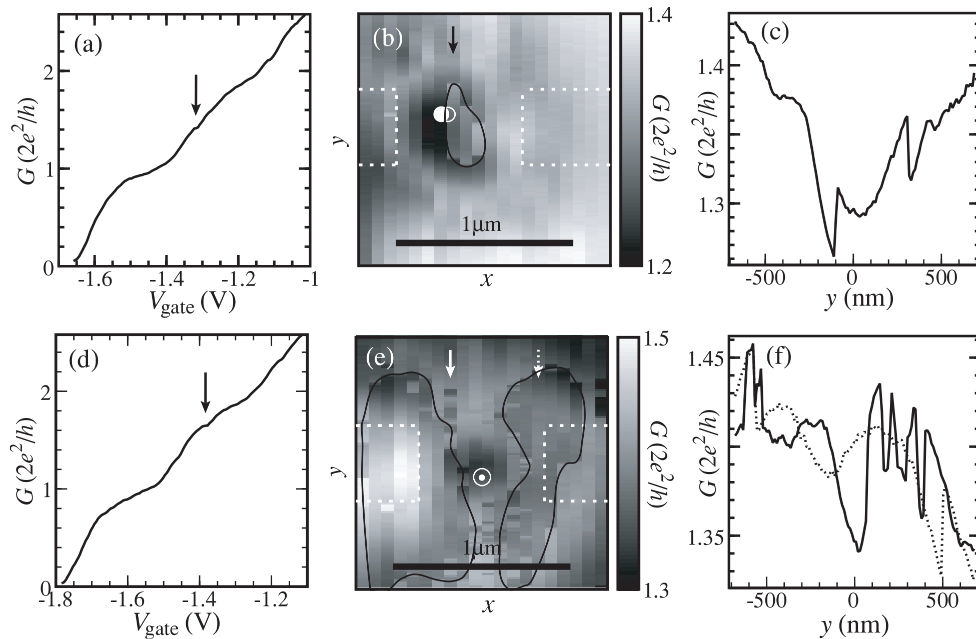

Figure 2. (a) Plot of Q1DES conductance against gate bias. (b) Conductance image exhibiting a distinct region of increased conductance. (c) Single sweep reproduced from image (b). (d-f) Corresponding plots and image made after a thermal cycle up to 77 K. The conductance image in (e) exhibits two regions of decreased conductance.

identified using an iterative approach to match theoretical contours of constant defect energy difference with tip position, to experimental contours generated by the switch. When the tip is positioned far from the Q1DES, one of the defect states, defined as the background defect state, is preferentially occupied. Occupation of the background defect state corresponds to the background region in the images, meaning the region outside that enclosed by the black line. In figure 2(b) the open white circle locates the background defect. This defect is closest to the Q1DES. The closed white circle locates the defect which is occupied to produce the central region of increased conductance. When the tip is positioned over this central region, the energies of the defect states are modified to favour electron tunnelling from the background defect to the defect causing increased conductance. The model defects are separated by 10.5 nm, which is similar to the effective Bohr radius in AlGaAs and of the order of the average dopant spacing.

General features of the images were found to be reproducible over several hours, but details at the switched region boundaries were not. Thermal cycling followed by illumination completely changed the features, but subsequent illumination did not. Figures 2(d), 2(e), and 2(f) show the same set of plots and images for the same device after heating to 77 K and then cooling back to 1.5 K, followed by illumination, with $V_{\mathrm{tip}} = -0.5$ V. The thermal cycle is unlikely to modify the donor positions, but will modify the detailed donor occupation. Figure 2(e) reveals two separate regions of decreased conductance. The approximate boundaries of the two regions of decreased conductance are identified by black lines. Figure 2(f) plots two single sweeps to include both such regions of figure 2(e), where they are identified by arrows. The energy change for the conductance step is approximately 100 μeV, and is equal for both regions. This suggests that all the switching seen in figure 2(e)

originates from the same defect system.

Unlike figure 2(b), the conductance decreases inside the switched regions in figure 2(e). Additionally, the switch appears to remain in the background state whenever the tip is positioned over the Q1DES or the nearby 2DES. An explanation is that this defect system is screened from the tip potential by a parallel layer of mobile electrons. Such a parallel layer, which need not be continuous, is caused by a high density of ionized donors in the doped AlGaAs layer bringing the conduction band below the Fermi level. Work involving a double 2DES has shown that screening from a parallel layer is possible despite an immeasurably small net current flow in the parallel layer [15]. The parallel layer is patterned by the gate electrodes to mirror the shape of the 2DES and Q1DES. If the defect system is located between the 2DES plane and the parallel layer then this image maps the Q1DES. Possible defect positions are again marked on the experimental image by an open white circle for the defect which is occupied to produce the background region and by a closed white circle for the defect which is occupied to produce the regions of decreased conductance. When the tip is positioned over depleted regions of the parallel layer, the tip potential is less well screened to raise the potential of the background defect relative to the defect causing reduced conductance. The defect causing reduced conductance is closer to the parallel conductivity layer and is therefore more effectively screened.

After further thermal cycles, the same device produced the conductance image shown in figure 3(a), with $V_{\text{tip}} = -1.5$ V. Structure in this image resembles multiple concentric halos. The separation between the halos increases radially outwards from near the Q1DES centre. Along a path from the Q1DES to the 2DES, electron energy increases and electron wavelength decreases. This rules out an electron interference effect as the origin of the halos.

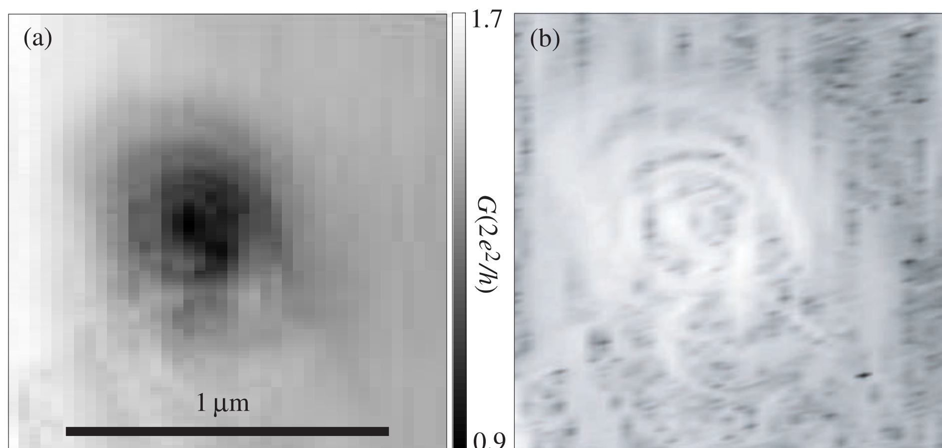

Figure 3. (a) Conductance image exhibiting concentric halos. (b) Image enhancement by removing low frequency background and interpolating between pixels.

Figure 3(b) is an image of the gradient $\left((\partial/\partial x)^2 + (\partial/\partial y)^2\right)^{0.5}$ of figure 3(a) followed by interpolation between the pixels. This enhances the image by removing the low-frequency background. Two sets of halos are revealed. One set of halos is centred over the Q1DES, and the other less distinct set is positioned lower in the image. Where the two sets of halos intersect they superimpose. The mechanism therefore originates in the device and not in the tip as an image of contours would then be expected.

Multiple occupancy switching is proposed as the origin of the halos. The energy states of

a single defect are too widely spaced to be responsible for this effect. A puddle of electrons located in the donor layer could be the cause of the halos, originating from either a highly doped region or a larger defect. Alternatively, a puddle of electrons could exist in the 2DES plane, but be isolated from the 2DES due to donor disorder as electron density is reduced in the proximity of the Q1DES [16]. Each halo signifies the addition of a single electronic charge to the puddle under the control of the tip position. The halos map lines of equal potential difference between the tip and the puddle.

In conclusion, we have shown that by combining conductance measurements of a sub-micron semiconductor device with the local electric field perturbation from a charged scanning tip, we are able to deduce information about the origin of a RTS in these devices. An electron hopping between defect states is consistent with the observed changes in electric potential at the device centre. This allowed the approximate defect locations to be calculated.

We acknowledge financial support from the EPSRC and the RW Paul Instrument Fund.

References

[1] Cobden D H, Patel N K, Pepper M, Ritchie D A, Frost J E F and Jones G A C 1991 *Phys. Rev.* B **44** 1938

[2] Cobden D H, Savchenko A, Pepper M, Patel N K, Ritchie D A, Frost J E F and Jones G A C 1992 *Phys. Rev. Lett.* **69** 502

[3] Sakamoto T, Nakamura Y and Nakamura K 1995 *Appl. Phys. Lett.* **67** 2220

[4] Sakamoto T, Nakamura Y, Sungwoo H and Nakamura K 1995 *Japanese J. Appl. Phys.* **34** 4302

[5] Eriksson M A, Beck R G, Topinka M, Katine J A, Westervelt R M, Campman K L and Gossard A C 1996 *Appl. Phys. Lett.* **69** 671

[6] Crook R, Smith C G, Barnes C H W, Simmons M Y and Ritchie D A 1999 *Proc. 24th Int. Conf. on The Physics of Semiconductors (Jerusalem)* ed D Gershoni (Singapore: World Scientific) p 190

[7] Crook R, Smith C G, Barnes C H W, Simmons M Y and Ritchie D A 2000 *J. Phys.: Condens. Matter* **12** L167

[8] Crook R, Smith C G, Simmons M Y and Ritchie D A 2000 *Phys. Rev.* B **62** 5174

[9] Topinka M A, LeRoy B J, Shaw S E J, Heller E J and Westervelt R M 2000 *Science* **289** 2323

[10] Field M, Smith C G, Pepper M, Ritchie D A, Frost J E F, Jones G A C and Hasko D G 1993 *Phys. Rev. Lett.* **70** 1311

[11] Tortonese M, Barret R C and Quate C F 1993 *Appl. Phys. Lett.* **62** 834

[12] Sellwood A T, Smith C G, Linfield E H and Simmons M Y 2001 *Rev. Sci. Instrum.* to be published

[13] Hauke M, Jakumeit J, Krafft B, Nimtz G, Förster A and Lüth H 1998 *J. Appl. Phys.* **84** 2034

[14] Thomas K J, Simmons M Y, Nicholls J T, Mace D R, Pepper M and Ritchie D A 1995 *Appl. Phys. Lett.* **67** 109

[15] Field M, Smith C G, Pepper M, Brown K M, Linfield E H, Grimshaw M P, Ritchie D A and Jones G A C 1996 *Surf. Sci.* **362** 154

[16] Nixon J A and Davies J H 1990 *Phys. Rev.* B **41** 7929